Peer-reviewed version available at Materials 2017, 10, 12; doi:10.3390/ma10010012

Article

Optically Clear and Resilient Free-Form μ-Optics 3D-Printed via Ultrafast Laser Lithography

Linas Jonušauskas [1,*], Darius Gailevičius [1], Lina Mikoliunaitė [2], Danas Sakalauskas [2], Simas Šakirzanovas [2], Saulius Juodkazis [3,4,*] and Mangirdas Malinauskas [1,*]

1 Department of Quantum Electronics, Faculty of Physics, Vilnius University, Saulėtekio Ave. 10, Vilnius LT-10223, Lithuania; darius.gailevicius@ff.vu.lt
2 Department of Applied Chemistry, Vilnius University, Naugarduko Str. 24, Vilnius LT-03225, Lithuania; lina.mikoliunaite@chf.vu.lt (L.M.); danas.sakalauskas@chf.vu.lt (D.S.); simas.sakirzanovas@chf.vu.lt (S.Š.)
3 Center for Micro-Photonics, Faculty of Engineering and Industrial Sciences, Swinburne University of Technology, Hawthorn VIC 3122, Australia
4 Melbourne Center for Nanofabrication, Australian National Fabrication Facility, Clayton VIC 3168, Australia
* Correspondence: linas.jon@gmail.com (L.J.); sjuodkazis@swin.edu.au (S.J.); mangirdas.malinauskas@ff.vu.lt (M.M.)

Abstract: We introduce optically clear and resilient free-form micro-optical components of pure (non-photosensitized) organic-inorganic SZ2080 material made by femtosecond 3D laser lithography (3DLL). This is advantageous for rapid printing of 3D micro-/nanooptics, including their integration directly onto optical fibers. A systematic study on the fabrication peculiarities and quality of resultant structures is performed. Comparison of microlenses' resiliency to CW and femtosecond pulsed exposure is determined. Experimental results prove that pure SZ2080 is ~3 fold more resistant to high irradiance as compared with a standard photo-sensitized material and can sustain up to 1.91 GW/cm^2 intensity. 3DLL is a promising manufacturing approach for high-intensity micro-optics for emerging fields in astro-photonics and atto-second pulse generation. Additionally, pyrolysis is employed to shrink structures up to 40% by removing organic SZ2080 constituents. This opens a promising route towards downscaling photonic lattices and creation of mechanically robust glass-ceramic structures.

Keywords: direct laser writing; ultrafast laser; 3D laser lithography; 3D printing; hybrid polymer; integrated microoptics; optical damage; photonics; pyrolysis; ceramic 3D structures

1. Introduction

Lithography oriented hybrid organic-inorganic polymers emerged as great materials for fabrication of objects in both 2D and 3D configurations [1–3]. They are choice material for 3D femtosecond laser structuring due to several convenient features. Those include optical transparency in the visible part of the spectrum [4] and use of photoinitiators absorbing the UV radiation [5–7]. Later makes them perfectly suitable for multiphoton polymerization [5,8] achieved by ultrafast laser and employed in true free-form structuring by 3D laser lithography (3DLL) [9]. Additionally, their refractive index and mechanical properties can be tuned by changing proportion between organic and inorganic part [4]. This led to extensive research in this area and, to date, new hybrid materials containing Si [1], Zr [4] and Ge [10] were made for 3DLL.

The Zr containing hybrid photopolymer, mostly refereed to as SZ2080, is especially interesting. It combines all the best properties offered by such materials, such as low shrinkage, hard gel form during fabrication, transparency for visible light [4] and thus is widely used in creation of structures to be employed in various applications in medicine [11], microoptics [12] and photonics [13]. In standard 3DLL case, photopolymerization of this material is initiated by the nonlinear absorption in the photoinitiator molecule [14]. However, recent works showed that photopolymerization in SZ2080 can be achieved without photoinitiator using both tight focusing, provided with high numerical

aperture (NA) objective, (NA>1) and loose (NA<1) focusing [15,16]. It is considered that such reaction is induced, when the nonlinear absorption takes place, which initiates braking of chemical bonds. Generated quasi-free electrons are subsequently accelerated by the intense electric field and provides bond cleavage via avalanche ionization [16,17]. This combination of multiphoton and avalanche ionization is responsible for subsequent crosslinking, which allows to form 3D microstructures out of pure material. Currently it is known that SZ2080 in its pure form is biocompatible [11] and has a high optical damage threshold [18].

This paper aims at expanding knowledge of 3DLL of pure SZ2080. Special attention is given to possible application in the field of microoptics. Thus, experiments for determining properties of pure SZ2080 relevant to this field are carried out. Results are compared to those obtained with photosensitized SZ2080. Functional microoptical elements are manufactured and their resilience to CW and femtosecond light exposure are tested. Furthermore, by applying pyrolysis we remove the organic part of the hybrid material leaving structures composed mainly of the glass-ceramic part. Finally, a pyrolysis induced shrinkage is employed in a controlled manner to create periodic latices consisting of thin (∼170-nm-wide) sintered rods.

2. Results

First, fidelity of 3D structuring of SZ2080 with and without photo-initiator was studied and micro-lenses were fabricated. Then, a comparative study of micro-lens performance in high irradiance was carried out down to structural degradation level. Finally, rescaling by sintering via pyrolysis to retrieve glass-ceramic 3D structures with significant 40% size reduction was studied.

2.1. Comparison of structuring properties

In 3DLL a well chosen photoinitiator (PI) can improve fabrication throughput and structure qualities for a material used [6,7,19–21]. The set of fabrication parameters needed for structuring material is generally refereed as fabrication window. In the simplest case it can be considered as range of intensities at some fixed translation velocity at which good quality structures are produced. Fabrication window is relatively wide (from ∼0.35 to ∼1.4 TW/cm^2 at translation velocities in range of hundreds μm/s) for SZ2080 when photosensitized with 1 wt% Irgacure 369 (IRG). Conventional thinking would let us to believe, that foregoing photosensitization would lead to absence of absorption completely preventing photopolymerization or hindering it to the point of heavily inefficient crosslinking and narrow fabrication window. In order to determine if that is the case we designed an experiment in which an array of identical structures was fabricated by varying the translation velocity and average laser power/peak intensity as these are the two parameters that are the most practical to change during fabrication. Structure chosen for this experiment was a cube with integrated single suspended lines. With such configuration it is possible to determine several important factors. First, such array provides information about the size of fabrication window by providing structure survival rate dependent on the set of parameters used. The cube shows if it is possible to structure true 3D structures. Finally, single lines give the possibility to measure fabricated feature sizes in transverse (d) and longitudinal (l) directions. For this reason it is called a *resolution array*. Outlined result showing fabrication windows achieved with such experiment is shown in Figure 1.

Result provided in Figure 1 shows several important features of pure SZ2080 in comparison to that containing PI. Although, threshold intensity required to polymerize pure material is higher by about $I_{P=80}$ - $I_{P=40}$ = 0.34 TW/cm^2, overall width of a fabrication window is comparable to that of polymer containing PI. By counting sectors in which structures are of the best quality we conclude that pure material provides only a 12.5% lesser structure survival rate compared to that of photosensitized polymer. Also, the photoinitiator containing polymer provides structures that maintain initial structural features even if parts of the structure are greatly affected by the defects caused by the overexposition, while in the case of objects formed from pure material completely

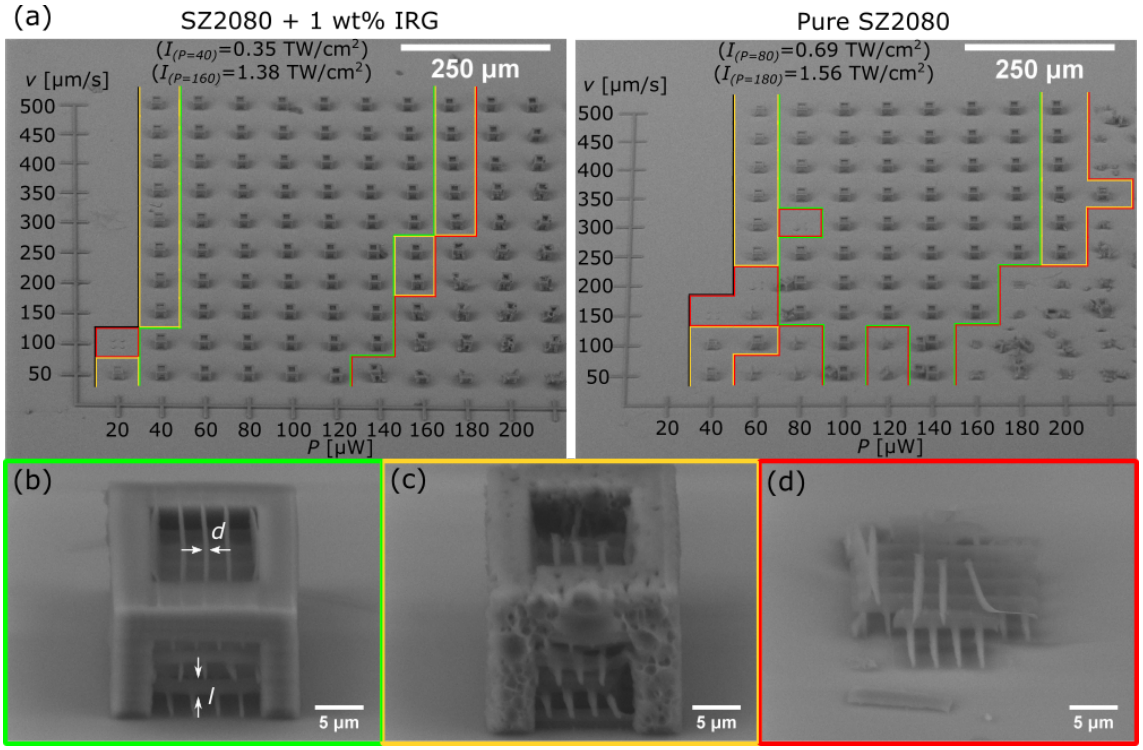

Figure 1. (a) SEM images of resolution arrays of photosensitized (left) and non-photosensitized (right) SZ2080. Structures with severe structural damage (red), with poor (yellow) and good (green) quality are outlined. Structure is considered good if internal single lines are observable and the shape of the cube is as designed. Average laser powers of the bottom and the top of the fabrication window are recalculated to the peak intensity (shown at the top). (b) One of the good quality structures in the array is shown in a greater detail; l and d marks longitudinal and transverse sizes of the lines. (c) The example of a poor quality structure and (d) the failed one.

collapse if non-optimal parameters are used [Figure 2 (a)]. This hints that without photoinitiator the crosslinking process is not as efficient and provides a final polymer matrix that considerably weaker. This result coincides well with other works showing that degree of crosslinking during 3DLL is essential for mechanical and optical properties of finished structures [22,23]. However, despite this, if fabrication parameters are within the fabrication window even advanced microoptical elements, like suspended microlenses on a tip of a optical fiber, can be fabricated out of pure material [Figure 2 (b)].

Dimensions of the lines inside cubes were measured. Case of translation velocity v = 250 μm/s was chosen as it is in the middle of the tested range in both photosensitized and non-photosensitized materials. It revealed that both transverse and longitudinal line dimensions are smaller in pure SZ2080 [Figure 3 (a)]. This correlates well with earlier findings [17]. It also reveals that features produced out of photosensitized material easily exceed the calculated spot size. On the other hand lines produced out of pure SZ2080 are all about the same size as the focus spot. This can be explained by the fact that photochemical chain reactions, in the case of photosensitized material, can expand more easily out of the volume in which nonlinear absorption took place. In case of pure resist, such process is less prominent. Also, the aspect ratios of formed voxels are very similar [Figure 3 (b)], thus showing that non-photosensitized material does not provide any benefit in control of the aspect ratio of a voxel. To better illustrate this we provide data for the line aspect ratio for 500 μm/s writing speed in Figure 3 (b).

Preprints (www.preprints.org) | NOT PEER-REVIEWED | Posted: 1 November 2016 doi:10.20944/preprints201611.0001.v1

Peer-reviewed version available at Materials 2017, 10, 12; doi:10.3390/ma10010012

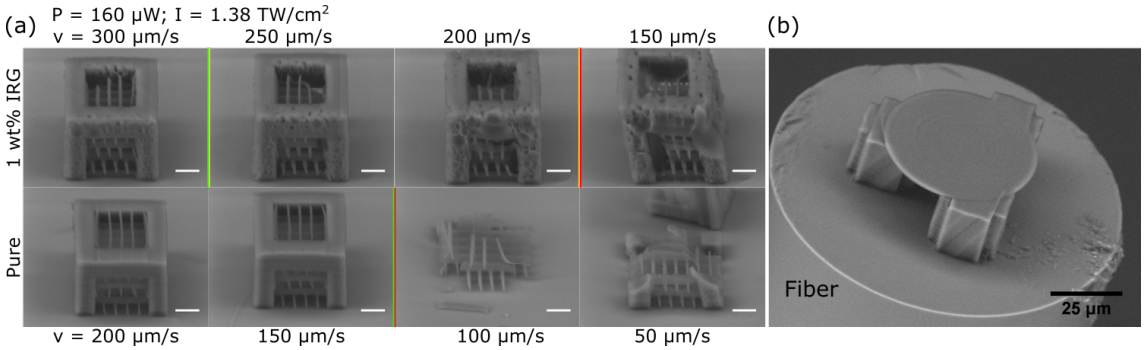

Figure 2. (a) Reduction of structural quality in case of photosensitized and pure SZ2080. While IRG containing cubes degrade slower and in more progressive fashion. On the contrary, the structures out of non-photosensitized material completely breaks as soon as parameters for fabrication are not in the fabrication window. All scales are 5 μm. (b) Monolithic microoptical element on a tip of a optical fiber fabricated out of non-photosensitized SZ2080.

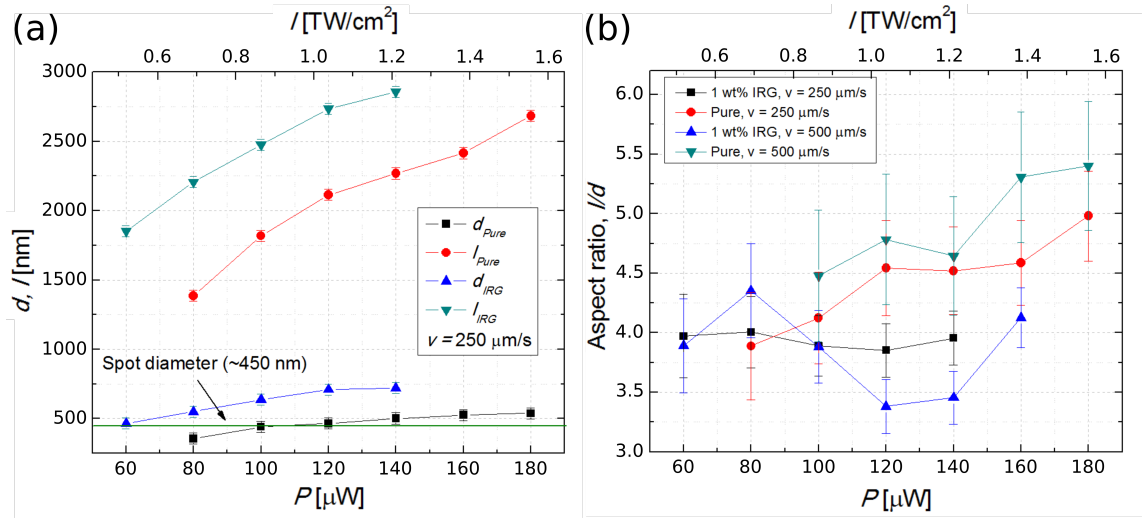

Figure 3. (a) Feature width d and height l measured in the resolution array at writing speed of 250 μm/s. (b) Aspect ratio of lines produced for cases of 250 μm/s and 500 μm/s speeds.

2.2. Surface roughness

Considering the application of SZ2080 for microoptics another important parameter is the surface quality of the final structures. There are several ways to quantify this property using data from precision measurement tools, such as a atomic force microscope (AFM) or very high magnification (∼50k<) scanning electron microscope (SEM). The most common way to evaluate measured surface elevations is the standard root mean square (RMS) which was chosen for this study. It is a common knowledge that if surface roughness of material is higher than $\lambda/8$ it is considered that surface quality is insufficient for use in optics. One the other hand, if roughness is smaller than $\lambda/20$ such material is considered suitable for optical applications. We are assuming microoptical elements to be designed for the use in visible part of spectrum, thus the lowest operational λ was chosen as 400 nm. AFM was employed to measure the surface profile of both pure and photosensitized SZ2080 samples. The geometry was of a flat square slab with side length of 100 μm [Figure 4 (a)]. Several different values of transverse voxel overlap (dx) were used to establish at which condition it was sufficient to achieve optical grade quality of the finished structure. It is important to note, that our goal was to determine if optical grade surface quality can be achieved at all with parameters similar to those applied in microlens fabrication and, if so, is it easier to obtain it with photosensitized or pure polymer. For

Preprints (www.preprints.org) | NOT PEER-REVIEWED | Posted: 1 November 2016 doi:10.20944/preprints201611.0001.v1

Peer-reviewed version available at Materials 2017, 10, 12; doi:10.3390/ma10010012

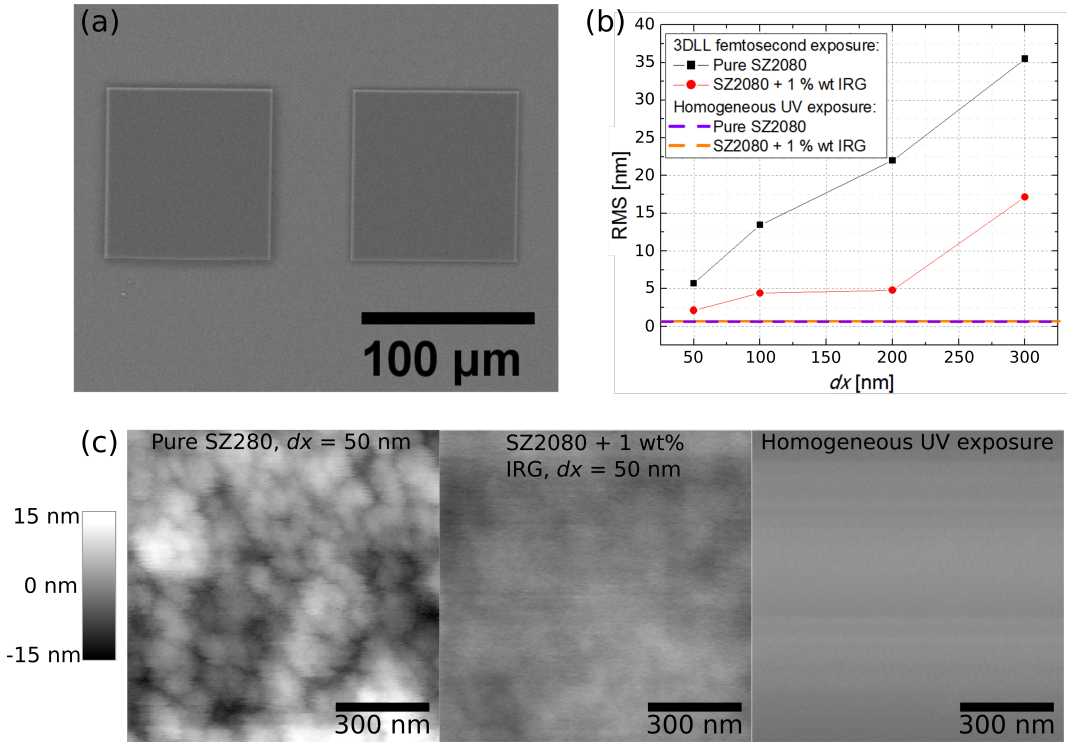

Figure 4. (a) SEM micrograph of the measured square polymerized structures. (b) AFM images of surfaces of the pure and photosensitized polymer obtained with highest voxel overlap (dx = 50 nm) as well as one which was produced via homogeneous UV exposure. (c) RMS calculated for surfaces fabricated with different dx for SZ2080 containing photoinitiator and in without it.

a control/comparison we used slab produced with one photon polymerization via homogeneous radiation of IV harmonic of Nd:YAG laser (λ = 258 nm) [18].

Both polymers had surface acceptable for optical applications. The IRG containing material allows to achieve surface roughness of RMS < 20 nm with smaller voxel overlap (dx = 300 nm, RMS = 17.1 nm), while in case of pure polymer required dx is 100 nm (RMS = 13.5 nm) [Figure 4 (b)]. The femtosecond laser structured pure SZ2080 is inherently more rough. Even at dx = 50 nm, when surface details of photosensitized SZ2080 becomes smooth, a non-photosensitized resist still exhibits a clear of nanofringes [Figure 4 (c)]. This could be explained by the fact, that with the non-photosensitized SZ2080 the polymerization mechanism is more chaotic, due to different and random process initiation pathways, compared to photosensitized sample. It would also explain why such microstructures lose mechanical integrity much quicker when applied parameters are out of fabrication window. It should be noted that difference in roughness is induced by employing 3DLL as control samples of both IRG containing and pure SZ20820 polymerized by UV radiation showed same flatness with RMS being less than 1 nm.

2.3. Resilience of microoptic s to high irradiance

Next, we tested how functional microoptical elements would perform under different light radiation conditions. It is known, that pure SZ2080 should have higher optical damage threshold when thin films characterized by standard laser induced damage threshold (LIDT) [18]. However, it is still unclear how this translates into operation of standard microlenses both qualitatively and quantitatively.

First, experiment was carried out with CW λ = 405 nm laser operating at average power of ~17 mW. Laser beam was focused to a ~250 μm radius spot onto 50 μm diameter microlenses, resulting in I = 86.6 W/cm^2. The microlenses were produced following procedure described

Peer-reviewed version available at Materials 2017, 10, 12; doi:10.3390/ma10010012

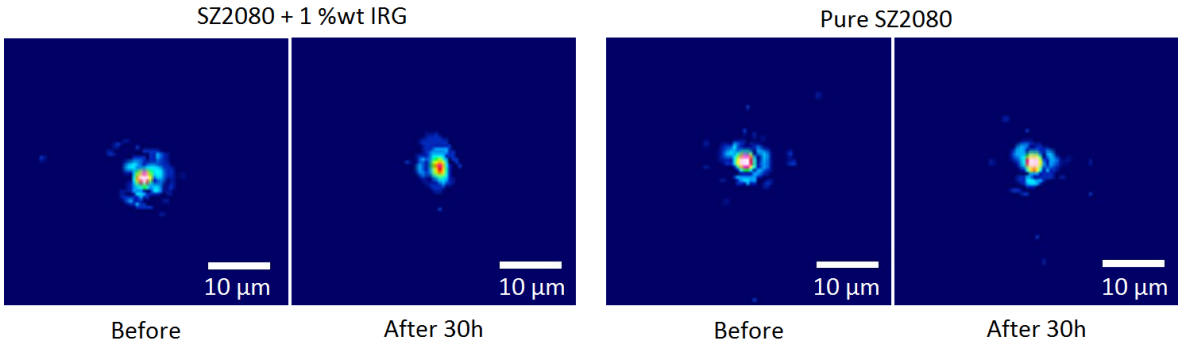

Figure 5. Images of microlens' focal plain before and after 30 h of exposure to 405 nm CW laser radiation. No significant change in the image at the focal point can be discerned.

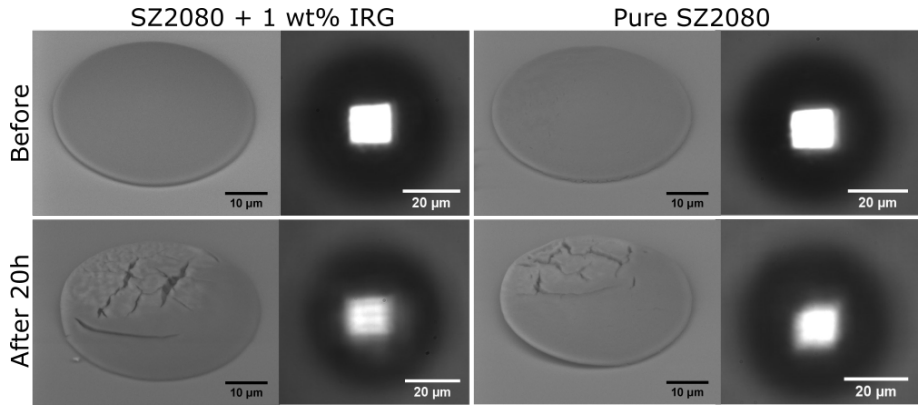

Figure 6. SEM images of microlenses before and after 20 h exposition to a loose focusing of 515 nm femtosecond laser radiation and image of a LED made by the lens. Degradation of a lateral light distribution in the focal plain can be seen both in the structural quality of the lenses and degraded projected image. The photoinitiator containing microlenses were more degraded.

earlier [24]. Intense laser radiation might induce changes both in the volume and on the surface of the microoptical element. For this reason focusing properties prior and after exposure to a potentially damaging light irradiation were examined using CCD camer to determine whether microlenses were affected. Microlenses were left in 405 nm light for 30 hours. Light source used to measure focusing properties of microlenses in this experiment was HeNe laser. As shown in Figure 5 with CW UV laser operating at 405 nm wavelength no effects on the focusing were observed.

Next, microlenses were left for 20 hours exposed to a pulsed laser beam operating at 300 fs, 200 kHz and 515 nm wavelength. The microfabrication setup was applied for this experiment, because it offered possibility of both controlling the femtosecond laser beam irradiation parameters and to simultaneously monitor focusing of the microlenses via built-in microscope. $40^{\times}$ $NA = 0.95$ objective was employed for imaging microlenses as well as to provide focusing for 515 nm radiation. An LED was imaged through the lenses as an illumination source. Objective was retracted 85 μm from being directly focused to the microoptical elements thus allowing laser beam to expand and to form a laser beam spot of $\sim$ 250 μm radius. Furthermore, it was deliberately offset in the transverse direction by 55 μm from the center of microlenses in order to see if damage to microlenses would depend on the intensity of the laser beam. Such prolonged exposure to femtosecond laser pulses resulted in severely damaged microlenses, that showed changes in focusing properties and overall integrity of the structure [Figure 6]. This investigation of micro-lens focusing shows that a microoptical element made out of pure SZ2080 was less damaged.

Preprints (www.preprints.org) | NOT PEER-REVIEWED | Posted: 1 November 2016 doi:10.20944/preprints201611.0001.v1

Peer-reviewed version available at Materials 2017, 10, 12; doi:10.3390/ma10010012

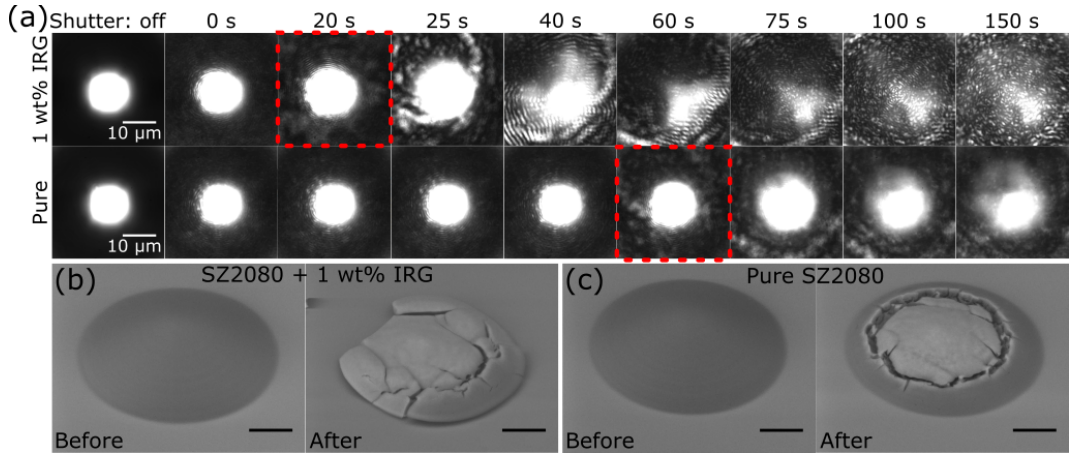

Figure 7. (a) Real time monitoring of a lateral intensity distribution of LED through microlenses produced using photosensitized and pure SZ2080 during irradiation with 515 nm/300 fs pulses at 200 kHz with peak intensity of 1.91 GW/cm^2 (spot radius of 100 μm). Faster degradation of SZ2080 containing 1 %wt IRG as compared with pure SZ2080 is evident, as image at the focus start to degrade after 60 and 20 s (marked by red dashed squares), respectively. (b) and (c) SEM micrographs of the tested lenses before and after exposure. The photosensitized element is entirely destroyed, while the one produced out of pure SZ2080 exhibits relatively low damage. Scale bars 10 μm.

In order to determine whether microoptical elements of pure SZ2080 are indeed more resilient to intense laser radiation a following time dependent experiment was carried out. We used 100$^\times$ $NA = 0.9$ objective to in situ monitor changes in the focal plain of the microlenses. As the objective was retracted 50 μm from the microlenses, $\sim$100 μm radius laser beam spot was formed, with its peak intensity of 1.91 GW/cm^2. Such exposure resulted in fast degradation of the image [Figure 7 (a)]. Two steps were discernable: when lens degradation becomes observable and when the LED image becomes completely obscured. In the case of IRG containing lens, deterioration started after 25 s of irradiation and caused total destruction after 35 s. In the case of pure SZ2080 microlenses, the time period till beginning of deterioration was 75 s and 100 s to fully obscured LED image. Hence, microlens made out of pure SZ2080 can withstand a $\sim$3 times larger exposure dose. Furthermore, the damage to the microlenses differed. Entire microlens was structurally damaged in the case of SZ2080 with 1 wt% IRG [Figure 7 (b)] resembling a thermomechanical failure, while pure SZ2080 lenses were damaged only in the central region by a homogeneous melting [Figure 7 (c)]. This shows that a polymer without a photoinitiator is clearly more resilient to the intense femtosecond laser exposure.

Presented analysis show degradation of micro-lenses during exposure. Whether it is caused by accumulated dose, or when critical temperature is reached was not established. Next, one set of lenses were continuously exposed for 15 min to 1.27 GW/cm^2 intensity radiation while the other set was irradiated for a combined 15 min exposure delivered in 10 s light bursts followed by 10 s pauses. This resulted in microlenses being severely damaged for both pure and photosensitized SZ2080 when exposed in continuous manner[Figure 8 (a)]. However, the multi-burst exposure of non-photosensitized microlenses showed no noticeable distortions, while the photosensitized lenses were noticeably degraded [Figure 8 (b)]. This clearly demonstrates that in the case of pure SZ2080 the cause of damage is the heat accumulated in the volume of the lens. A better mitigation of heat load could solve thermal degradation of microoptical elements.

2.4. Freeform ceramic structures out of pyrolysed SZ2080

Despite being more rigid and optically resilient in comparison to standard photopolymers [18], hybrid materials still have the limitations imposed by their organic part. On the other hand, organic part is the reason why freeform laser nano-structuring is possible. Recent developments

Peer-reviewed version available at Materials 2017, 10, 12; doi:10.3390/ma10010012

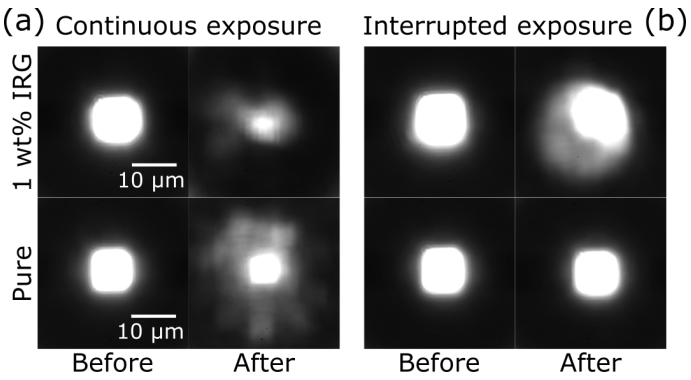

Figure 8. Focusing performance of microlenses after exposure to I = 1.27 GW/cm^2 in continuous (a) and multi-burst mode: 10 s exposure followed by a 10 s pause (b).

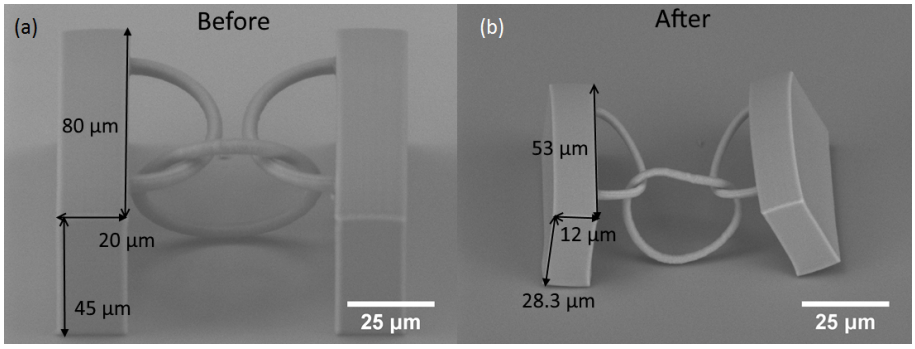

Figure 9. SEM images of the structure consisting of supporting walls and free hanging ring before (a) and after (b) pyrolysis; magnification is the same. Fabricated objects appears brighter after pyrolysis, which indicates a change in the electrical conductivity of material.

in the field of material processing showed, that hybrid materials can be processed via pyrolysis by removing the organic part and leaving only the ceramic structure. It was successfully demonstrated using stereolithography at a millimeter-scale [25,26] or at smaller scale using commercially available photoresists [27,28]. Here we show a similar result in the micro- and nano-scales for SZ2080.

The initial sample structures chosen for the experiment were thick supporting walls with free hanging chain between them [Figure 9 (a)]. Resulting structures shrunk to about 65% of the initial dimensions [Figure 9 (b)]. The free hanging ring shrunk and deformed unevenly during pyrolysis. Peeling of supporting structures from the substrate was observed.

Next, pyrolysis is employed to tailor photonic crystals with ultra-thin lines. Photonic crystals designed to operate in visible part of the spectrum require their resolution to be sub-wavelength [29]. 3DLL allows to achieve needed feature sizes [30,31], yet it is relatively problematic due to necessity to use ultra-short (< 100 fs) laser pulses, tight focusing with oil-immersion lenses, and complicated post processing techniques, such as critical point drying [32]. Here we produce woodpile photonic crystals with line widths that can be achieved without any additional post processing and then reduce them in size by the application of pyrolysis. Line widths of 295±25 nm [Figure 10 (a)] were changed to 174±15 nm [Figure 10 (a)], which is reduction of about ∼40%. The processed structure retained its overall shape. It is demonstrated by the ratio between photonic crystal period and line width retaining the same ∼1.7 value before and after pyrolysis. Therefore this technique does not require complicated compensation algorithms to be used during laser writing.

In order to gain further insights at what happens during pyrolysis, a thermal gravimetric analysis (TGA) of a drop of unprocessed SZ2080 was performed [Figure 11]. First, sudden decrease in weight at 100°C can be attributed to evaporation of solvent which otherwise would be removed during

Peer-reviewed version available at Materials 2017, 10, 12; doi:10.3390/ma10010012

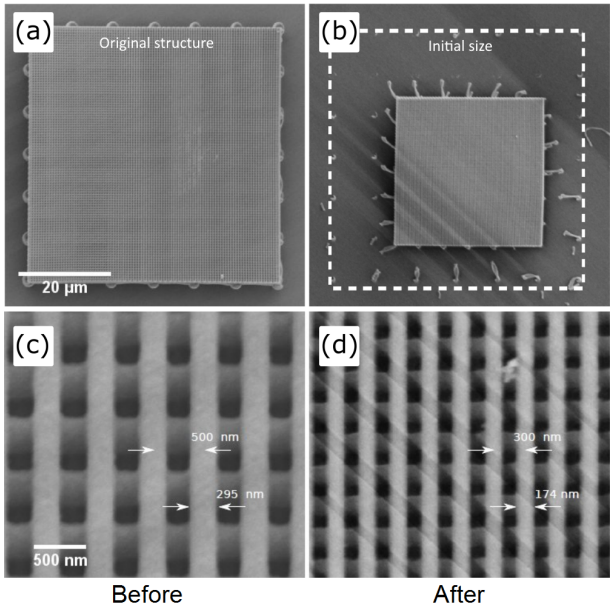

Figure 10. (a) SEM micrograph of a photonic crystal prior (a) and after (b) pyrolysis. (c) The period and line width initially were 500 nm and 295 nm, respectively, which were shrunk to 300 nm and 174 nm after pyrolysis (d); a change of ∼40%. The *period*/*width* ratio stayed ∼1.7 indicating a homogeneous reduction in size.

pre-bake. The weight then remains relatively stable up until temperature reaches 350°C, when it starts to decrease again. The organic part of the hybrid is decomposed at this stage. During this period two distinct changes in the decrease of weight are discerned hinting at two distinct phases in which organic part of the material is removed from the hybrid. A change in weight was about 28%. This exceeded the volume change of ∼35-40% and indicates that lost part of the material is relatively low density organic compounds. Also, it is assumed that the remaining material is densified resulting in a shrunken ceramic structure.

3. Discussion

Here we discuss the 3DLL of pure materials in details. First femtosecond laser photopolymerization of a SZ2080 with IRG photoinitiator is recalled. Light breaks weak single bonds of photoinitiator molecule, which then creates two radicals PI* [Figure 12 (a) (1)-(2)] (a) [17]. These radicals then react with pre-polymer molecules via double bonds creating radicalized monomer SZ* [Figure 12 (a) (3)-(4)]. This initiates a chain reaction and growth of an intertwined polymer matrix, which does not dissolve in the organic solvent. In the case of a SZ2080 without photoinitiator, such reaction is induced when nonlinear absorption occurs. The double bond is broken in the pre-polymer [Figure 12 (b) (1)-(2)], which otherwise would be broken by reaction with photoinitiator molecule. Taking that laser induced multiphoton excitation rate of pre-polymer species is high in comparison to the thermalization rate which can be as long as $\sim 10^{-6}$ seconds [33], meaning that large excitations can build up in the intermediary states. Photochemical (photolytic) processes are dominant compared to photothermal phenomena due to absence of detectable thermal effects, such as sample vaporization, boiling or thermal expansion. High irradiance exposure is sufficient to directly break chemical bonds of pre-polymerized SZ2080 organic constituents, which initialise formation of insoluble and rigid organic-inorganic composite.

With ever increasing demand for advanced optical elements in optical systems, freeform 3D microstructuring techniques become more sophisticated. While advanced glass processing techniques show some possibilities to produce relatively small (∼nm-μm) structures [34], it still

Preprints (www.preprints.org) | NOT PEER-REVIEWED | Posted: 1 November 2016 doi:10.20944/preprints201611.0001.v1

Peer-reviewed version available at Materials 2017, 10, 12; doi:10.3390/ma10010012

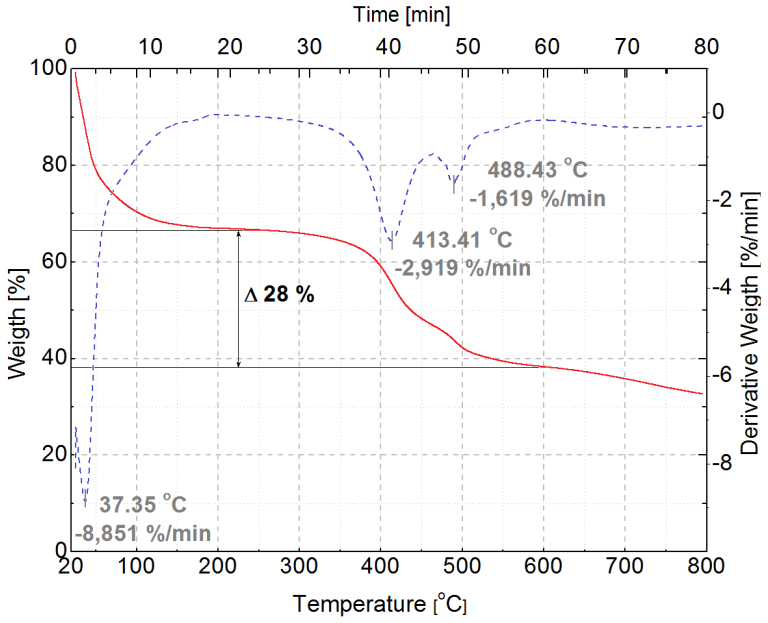

Figure 11. TGA data showing weight lost vs temperature. A weight loss was 28%; an observed shrinkage was ∼40%. The organic part was decomposed and removed by pyrolysis.

lacks in surface quality and a capability to perform true 3D fabrication. To date, only direct laser writing based 3DLL was shown to be capable of true 3D manufacture at the microscale. This additive manufacturing technique [35] combines a complete freedom of architecture of produced structures [36], possibility to integrate it on various substrates [37–39] and a large range of materials that can be processed in such fashion [40]. Here we have shown that structures produced out of zirconium containing photopolymer SZ2080 can withstand a relatively low intensity $I = 86.6\ \mathrm{W/cm^2}$ short wavelength exposure for prolonged time periods. It was shown that microoptical elements made out of SZ2080 have good resilience to high repetition rate femtosecond laser radiation. This well matches with earlier findings of higher optical damage threshold of such SZ2080 [18]. Finally, we have shown that surface quality of structures produced from non-photosensitized and photosensitized SZ2080 has a low surface roughness (RMS $< \lambda/20$ at $\lambda < 400$ nm) and is suitable for applications in micro-optics and opto-fluidics [**?**].

Development of microoptical elements made from a high-purity glassy hybrid material via a simple low temperature chemical synthesis without use of photoinitiators, which are usually required for the light absorption, can help new developments in several fields. For high intensity laser applications, use of micro-optical elements has several distinct advantages due to optical damage scaling rules [41]: 1) the damage threshold decreases with increasing the the spot area $I_{dam} \propto 1/\sqrt{A_{spot}}$, 2) micro-optical elements have a low surface roughness, δ_{surf}, which increase the damage threshold $I_{dam} \propto 1/\delta_{surf}^{m}$ with the exponent m between 1 and 1.5. In the field of light filamentation of ultra-short laser pulses in air and gasses, an exploration of multiple beamlet generation apertures [42], ring Airy beams [43], realization of multifilaments – super-filamentation [44] is an active research area. The peak intensities on the beam forming optics can reach pre-breakdown intensities of several $\mathrm{TW/cm^2}$ which demands low absorption materials (no photoinitiators in polymerised microoptics) according to the scaling $I_{dam} = \frac{0.26\ \mathrm{MW/cm^2}}{(\alpha/\mathrm{cm^{-1}})^{0.74}}$, where absorption coefficient $\alpha = -1/L \ln(T)$ is defined by transmission T and propagation length L [41]. While microlenses have inherently low L, the result of removing photoinitiators also greatly minimizes T. This is the reason why small optical elements using refractive and diffractive beam forming concepts made from hight purity materials are the most promising candidates in high power laser field.

Peer-reviewed version available at Materials 2017, 10, 12; doi:10.3390/ma10010012

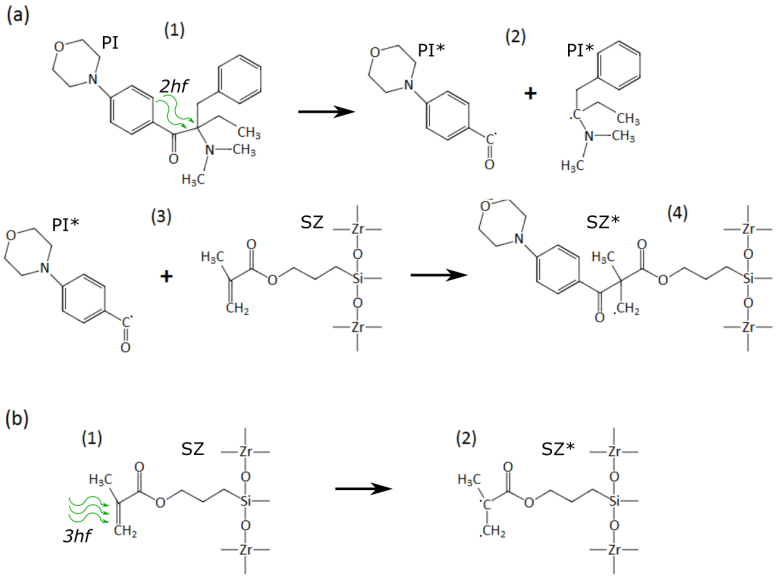

Figure 12. (a) Polymerization reactions initiated by nonlinear absorption of photoinitiator molecule and subsequent chemical pathways resulting in a cross linked SZ2080. (b) SZ2080 cross linking without photoinitiator.

The fact that material can be structured without photoinitiator with a fabrication window comparable to that of photosensitized material is a promising discovery for other science fields as well. Earlier studies dedicated to pure material structuring by femtosecond laser pulses [16,45] have shown to be complicated and slow. If such pure material can be structured at a relatively high speed (~mm/s) it would become suitable for biomedical applications, where structure dimensions are in the range of mm-cm [46]. Pure material would guarantee superb biocompatibility, which is a key requirement for tissue engineering. especially taking into account biodegradable implants.

For other diverse applications, SZ2080 can be doped with organic die molecules [47] or noble metal nanoparticles [48], which can be used for polymerisation control or increased functionalities. In the recently developed field of astro-photonics [49], where absorption in laser written waveguide lanterns is strong [50], the polymerised waveguides can tackle high loss problem. The photonic wire bonding also improves light confinement, flexibly control 3D conformation of fiber bundles for phase matched light delivery from the optical image plane to a spectrometer slit, and well defines a single-mode operation of the fiber by a precise control of polymerised wire cross section. Unexpectedly from prospective of high light intensity applications, a large volume optical astro-instrumentation is highly sensitive to detector background counts due radioactive trace elements in glass-optics. Potentially a better control of glass forming ingredients can be made in the case of photopolymer selection for optical elements prepared via a sol-gel route as SZ2080.

Composition control of sol-gel resists via different portions of organic and inorganic components provides a tool to tune refractive index and to create complex micro-optical elements for high quality optical imaging as compared with only shape control of composite lenses [38]. With pyrolysis, an even larger range of refractive index tunability is accessible. Current endoscopy and optical imaging applications where micro-optical elements are in contact with live tissue, would benefit from absence of photointiators due to a strong optical absorbance and bio-toxicity.

A possibility to use pyrolysis is an additional feature of SZ2080 due to its hybrid organic-inorganic nature to achieve true 3D glass ceramic structures is expected to open new applications. Shrinkage of the polymer [51] can be used to achieve ultra thin structures [52]. Further work aimed at pyrolysis control of SZ2080 will be basis for our future work.

4. Conclusions and Outlook

Detailed study of laser structuring of non-photosensitized SZ2080 via 3DLL was carried out. The photo-polymer has a fabrication window only 12.5% narrower than SZ2080 photosensitized with 1% IRG. Surface roughness of structures produced out of both compositions were in range of RMS < 2 nm which is sufficient for fabrication of micro-optical components. Structuring fidelity of both materials is comparable if parameters from within the fabrication window are used. Micro-optical element made out of pure SZ2080 was integrated on the tip of an optical fiber.

Furthermore, investigation of microoptical element degradation at various laser irradiations is performed. It is shown that SZ2080 in both photosensitized and pure forms are not damaged by tens of hours of exposure to CW 405 nm laser providing I = 86.6 W/cm^2. On the other hand, microlenses produced out of pure material was shown to survive ∼3 fold longer when irradiated by 515 nm 300 fs 200 kHz laser at 1.91 GW/cm^2 intensity. If intensity is dropped to 1.27 GW/cm^2 and delivered in interrupted manner (10 seconds of exposure fallowed by 10 second pause) non-photosensitized microlenses show no signs of degradation even after combined exposure of 15 min, while those containing IRG are damaged substantially. This indicates that in case of microlenses main deterioration inducing factor is thermo-accumulation and subsequent melting.

Additionally, pyrolysis of hybrid material was performed removing organic constitutes, leaving only densified glass-ceramic structure. Shrinkage during this process was homogeneous and allowed size reduction by 35-40%, which is a record high number. Further studies will be focused on optical and mechanical properties of glass-ceramics and its applications for a high irradiance optics and material processing with high-peak intensity of high-repetition rate conditions [**?** **?**]. Potential applications are in the fields of fillamentation of ultra-short laser pulses, fabrication of fiber-optical elements for sensor applications in chemically harsh, high temperature, and radioactive environments encountered in nuclear power stations and in optically driven inertial confinement fusion facilities.

5. Materials and Methods

SZ2080 photoresist was acquired from FORTH (Heraklion, Greece) and, as its name implies, contained 20%wt of inorganic and 80%wt of organic parts. For cross check experiments, SZ2080 was photosensitized by mixing it with 1%wt of a commercial photoinitiator Irgacure 369 (IRG). Samples were prepared by drop casting one droplet of the material on a glass substrate and then pre-backing sample at 75°C for 45 min. After fabrication, samples were developed in isobutyl methyl ketone for 45 min and subsequently rinsed in isopropanol for 15 min.

Schematics of the used 3DLL setup is shown in Figure 13. The fs-laser was Pharos (Light Conversion Ltd.) operating at 1030 nm fundamental wavelength, 300 fs pulse duration and 200 kHz repetition rate. Power is controlled with two power control units consisting of $\lambda/2$ waveplate and Brewster angle polarizer. Such two stage power attenuation allows to minimize power fluctuations and provides a precise power control during the fabrication. A second harmonics at 515 nm wavelength was used for 3D free-form polymerisation. Laser beam is expanded by 2$^\times$ magnification telescope in order to fill all the objective aperture. During experiments in which precise feature size control was essential (for instance a photonic crystal), polarization of incident light was kept at constant 45° degree angle with both horizontal translation axes, this way avoiding any polarization induced anisotropy of fabricated line widths [53]. Structure fabrication is performed with combination of Aerotech linear stages (ALS130-110-X,Y for positioning in XY plane, ALS130-60-Z for Z axis) and galvanoscanner, operating in sync in infinite field of view (IFOV) regime, which allows high fabrication speeds (∼mm/s) and superb structure quality. The sample is also illuminated by red LED which allows to monitor fabrication process in real time using CMOS camera.

Preprints (www.preprints.org) | NOT PEER-REVIEWED | Posted: 1 November 2016 doi:10.20944/preprints201611.0001.v1

Peer-reviewed version available at Materials 2017, 10, 12; doi:10.3390/ma10010012

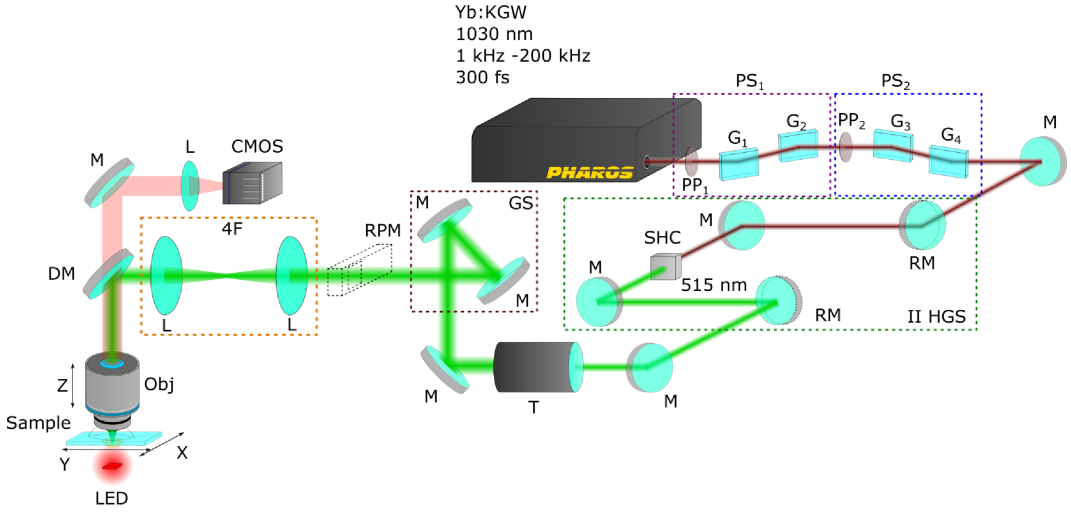

Figure 13. Fabrication setup used in this work: PS - power control stage, PP - phase plate, G - glass plate, M - mirror, RM - removable mirror, SHC - second harmonic crystal, T - telescope, GS - galvanoscanner, RPM - removable power meter, L - lens, 4F - lens system in 4F configuration, DM - dichroic mirror, CMOS - CMOS camera used to monitor fabrication process, Obj - objective lens, LED - LED used for sample illumination.

The average laser power P was first measured before polymerization experiments and was then recalculated to the peak intensity (I) at the center of focal point [15]:

$$I = \frac{2PT}{fw^2\pi\tau}, \tag{1}$$

where f is the pulse repetition rate, τ is the pulse duration, and $\omega = 0.61\lambda/NA$ is the waist (radius) of the beam. $T \simeq 0.41$ is the system transparency without glass substrate and pre-polymer for a $63^{\times}$ $NA = 1.4$ objective. Intensities used in the work are specified where applies. For microlenses, I_{IRG}=0.48 TW/cm^2, I_{pure}=0.61 TW/cm^2 using 50 μm/s translation velocity. For AFM analysis, structures were fabricated at I_{pure}=0.61 TW/cm^2 and I_{pure}=0.86 TW/cm^2 and translation speed of 250 μm/s.

Pyrolysis was perfromed in Ar atmosphere in 600°C temperature for 5 hours. All bulk and periodic microstructures were fabricated with parameters similar to those of AFM structures and were produced only out of pure SZ2080.

Surface roughness was characterized using SEM TM-1000 (Hitachi) and atomic force microscope (AFM) Catalyst (Bruker) with a gold coated SiN-needle with a k=0.06 N/m stiffness at F=18 kHz and with the tip diameter of 20 nm. For TGM, analysis Pyris 1 TGA (Perkin Elmer) equipment was used; sample was heated under nitrogen atmosphere from 30°C to 800°C with a heating rate 10°C/min.

Acknowledgments: Authors acknowledge ECs Seventh Framework Programme Laserlab-Europe IV JRA support BIOAPP (EC-GA 654148). DG, SJ and MM acknowledge NATO grant SPS-985048 "Nanostructures for Highly Efficient Infrared Detection".

Author Contributions: L.J. wrote the manuscript, designed and performed all the fabrication and optical element degradation experiments, did most of the measurements and evaluated received data; DG carried out pyrolysis of photonic crystals; L.M. contributed AFM measurements; D.S. carried out a high resolution SEM imaging of photonic crystals. S.Š. provided insights about pyrolysis and chemical reactions during photopolymerization processes; S.J. and M.M. proposed the direction and supervised the research. All the authors contributed to the editing of the manuscript.

Conflicts of Interest: The authors declare no conflict of interest.

Peer-reviewed version available at Materials 2017, 10, 12; doi:10.3390/ma10010012

References

1. Houbertz, R.; Frohlich, L.; Popall, M.; Streppel, U.; Dannberg, P.; Bräuer, A.; Serbin, J.; Chichkov, B. Inorganic-Organic Hybrid Polymers for Information Technology: from Planar Technology to 3D Nanostructures. *Adv. Eng. Mater.* **2003**, *5*, 551–555.
2. Serbin, J.; Egbert, A.; Ostendorf, A.; Chichkov, B.N.; Houbertz, R.; Domann, G.; Schulz, J.; Cronauer, C.; Fröhlich, L.; Popall, M. Femtosecond laser-induced two-photon polymerization of inorganic-organic hybrid materials for applications in photonics. *Opt. Lett.* **2003**, *28*, 301–303.
3. Lebeau, B.; Innocenzi, P. Hybrid materials for optics and photonics. *Chem. Soc. Rev.* **2011**, *40*, 886–906.
4. Ovsianikov, A.; Viertl, J.; Chichkov, B.; Oubaha, M.; MacCraith, B.; Sakellari, I.; Giakoumaki, A.; Gray, D.; Vamvakaki, M.; Farsari, M.; Fotakis, C. Ultra-Low Shrinkage Hybrid Photosensitive Material for Two-Photon Polymerization Microfabrication. *ACS Nano* **2008**, *2*, 2257–2262.
5. Schafer, K.J.; Hales, J.M.; Balu, M.; Belfield, K.D.; Van Stryland, E.W.; Hagan, D.J. Two-photon absorption cross-sections of common photoinitiators. *J. Photochem. Photobiol. A* **2004**, *162*, 497–502.
6. Rajamanickam, V.P.; Ferrara, L.; Toma, A.; Zaccaria, R.P.; Das, G.; Fabrizio, E.D.; Liberale, C. Suitable photo-resists for two-photon polymerization using femtosecond fiber lasers. *Microelectron. Eng.* **2014**, *121*, 135–138.
7. Harnisch, E.; Russew, M.; Klein, J.; Konig, N.; Crailsheim, H.; Schmitt, R. Optimization of hybrid polymer materials for 2PP and fabrication of individually designed hybrid microoptical elements thereof. *Opt. Mater. Express* **2015**, *5*, 456–461.
8. Lee, K.S.; Yang, D.Y.; Park, S.H.; Kim, R.H. Recent developments in the use of two-photon polymerization in precise 2D and 3D microfabrications. *Polymer. Adv. Tech.* **2006**, *17*, 72–82.
9. Sun, H.B.; Kawata, S. Two-Photon Photopolymerization and 3D Lithographic Microfabrication. In *NMR 3D Analysis Photopolymerization*; Springer Science + Business Media, 2006; pp. 169–273.
10. Malinauskas, M.; Žukauskas, A.; Purlys, V.; Gaidukevičiūtė, A.; Balevičius, Z.; Piskarskas, A.; Fotakis, C.; Pissadakis, S.; Gray, D.; Gadonas, R.; Vamvakaki, M.; Farsari, M. 3D microoptical elements formed in a photostructurable germanium silicate by direct laser writing. *Opt. Laser Eng.* **2012**, *50*, 1785–1788.
11. Mačiulaitis, J.; Deveikytė, M.; Rekštytė, S.; Bratchikov, M.; Darinskas, A.; Šimbelytė, A.; Daunoras, G.; Laurinavičienė, A.; Laurinavičius, A.; Gudas, R.; Malinauskas, M.; Mačiulaitis, R. Preclinical study of SZ2080 material 3D microstructured scaffolds for cartilage tissue engineering made by femtosecond direct laser writing lithography. *Biofabrication* **2015**, *7*, 015015.
12. Malinauskas, M.; Gilbergs, H.; Žukauskas, A.; Purlys, V.; Paipulas, D.; Gadonas, R. A femtosecond laser-induced two-photon photopolymerization technique for structuring microlenses. *J. Opt.* **2010**, *12*, 035204.
13. Sun, Q.; Juodkazis, S.; Murazawa, N.; Mizeikis, V.; Misawa, H. Freestanding and movable photonic microstructures fabricated by photopolymerization with femtosecond laser pulses. *J. Micromech. Microeng.* **2010**, *20*, 035004.
14. Farsari, M.; Vamvakaki, M.; Chichkov, B.N. Multiphoton polymerization of hybrid materials. *J. Opt.* **2010**, *12*, 124001.
15. Jonušauskas, L.; Rekštytė, S.; Malinauskas, M. Augmentation of direct laser writing fabrication throughput for three-dimensional structures by varying focusing conditions. *Opt. Eng.* **2014**, *53*, 125102.
16. Buividas, R.; Rekštytė, S.; Malinauskas, M.; Juodkazis, S. Nano-groove and 3D fabrication by controlled avalanche using femtosecond laser pulses. *Opt. Mater. Express* **2013**, *3*, 1674–1686.
17. Malinauskas, M.; Žukauskas, A.; Bičkauskaitė, G.; Gadonas, R.; Juodkazis, S. Mechanisms of three-dimensional structuring of photo-polymers by tightly focussed femtosecond laser pulses. *Opt. Express* **2010**, *18*, 10209–10221.
18. Žukauskas, A.; Batavičiūtė, G.; Ščiuka, M.; Jukna, T.; Melninkaitis, A.; Malinauskas, M. Characterization of photopolymers used in laser 3D micro/nanolithography by means of laser-induced damage threshold (LIDT). *Opt. Mater. Express* **2014**, *4*, 1601–1616.
19. Li, Z.; Torgersen, J.; Ajami, A.; Muhleder, S.; Qin, X.; Husinsky, W.; Holnthoner, W.; Ovsianikov, A.; Stampfl, J.; Liska, R. Initiation efficiency and cytotoxicity of novel water-soluble two-photon photoinitiators for direct 3D microfabrication of hydrogels. *RSC Adv.* **2013**, *3*, 15939.

20. Sakellari, I.; Kabouraki, E.; Gray, D.; Purlys, V.; Fotakis, C.; Pikulin, A.; Bityurin, N.; Vamvakaki, M.; Farsari, M. Diffusion-Assisted High-Resolution Direct Femtosecond Laser Writing. *ACS Nano* **2012**, *6*, 2302–2311.
21. Fischer, J.; Freymann, G.; Wegener, M. The Materials Challenge in Diffraction-Unlimited Direct-Laser-Writing Optical Lithography. *Adv. Mater.* **2010**, *22*, 3578–3582.
22. Jiang, L.; Xiong, W.; Zhou, Y.; Liu, Y.; Huang, X.; Li, D.; Baldacchini, T.; Jiang, L.; Lu, Y. Performance comparison of acrylic and thiol-acrylic resins in two-photon polymerization. *Opt. Express* **2016**, *24*, 13687–13701.
23. Žukauskas, A.; Matulaitienė, I.; Paipulas, D.; Niaura, G.; Malinauskas, M.; Gadonas, R. Tuning the refractive index in 3D direct laser writing lithography: towards GRIN microoptics. *Laser Photon. Rev* **2015**, *9*, 706–712.
24. Malinauskas, M.; Žukauskas, A.; Purlys, V.; Belazaras, K.; Momot, A.; Paipulas, D.; Gadonas, R.; Piskarskas, A.; Gilbergs, H.; Gaidukevičiūtė, A.; Sakellari, I.; Farsari, M.; Juodkazis, S. Femtosecond laser polymerization of hybrid/integrated micro-optical elements and their characterization. *J. Opt.* **2010**, *12*, 124010.
25. Schwentenwein, M.; Homa, J. Additive Manufacturing of Dense Alumina Ceramics. *Int. J. Appl. Ceram. Technol.* **2014**, *12*, 1–7.
26. Eckel, Z.C.; Zhou, C.; Martin, J.H.; Jacobsen, A.J.; Carter, W.B.; Schaedler, T.A. Additive manufacturing of polymer-derived ceramics. *Science* **2015**, *351*, 58–62.
27. Tétreault, N.; von Freymann, G.; Deubel, M.; Hermatschweiler, M.; Pérez-Willard, F.; John, S.; Wegener, M.; Ozin, G. New Route to Three-Dimensional Photonic Bandgap Materials: Silicon Double Inversion of Polymer Templates. *Adv. Mater.* **2006**, *18*, 457–460.
28. Li, J.; Jia, B.; Gu, M. Engineering stop gaps of inorganic-organic polymeric 3D woodpile photonic crystals with post-thermal treatment. *Opt. Express* **2008**, *16*, 20073.
29. Rill, M.S.; Plet, C.; Thiel, M.; Staude, I.; Freymann, G.; Linden, S.; Wegener, M. Photonic metamaterials by direct laser writing and silver chemical vapour deposition. *Nat. Mater.* **2008**, *7*, 543–546.
30. Haske, W.; Chen, V.W.; Hales, J.M.; Dong, W.; Barlow, S.; Marder, S.R.; Perry, J.W. 65 nm feature sizes using visible wavelength 3-D multiphoton lithography. *Opt. Express* **2007**, *15*, 3426–3436.
31. Wollhofen, R.; Katzmann, J.; Hrelescu, C.; Jacak, J.; Klar, T.A. 120 nm resolution and 55 nm structure size in STED-lithography. *Opt. Express* **2013**, *21*, 10831–10840.
32. Hengsbach, S.; Lantada, A.D. Direct laser writing of auxetic structures: present capabilities and challenges. *Smart Mater. Struct* **2014**, *23*, 085033.
33. Bäuerle, D. *Laser Processing and Chemistry*; Springer Nature, 2011.
34. Wortmann, D.; Gottmann, J.; Brandt, N.; Horn-Solle, H. Micro- and nanostructures inside sapphire by fs-laser irradiation and selective etching. *Opt. Express* **2008**, *16*, 1517.
35. Vaezi, M.; Seitz, H.; Yang, S. A review on 3D micro-additive manufacturing technologies. *Int. J. Adv. Manuf. Tech.* **2012**, *67*, 1721–1754.
36. Maruo, S.; Fourkas, J.T. Recent progress in Multiphoton microfabrication. *Laser Photon. Rev* **2008**, *2*, 100–111.
37. Lightman, S.; Gvishi, R.; Hurvitz, G.; Arie, A. Shaping of light beams by 3D direct laser writing on facets of nonlinear crystals. *Opt. Let.* **2015**, *40*, 4460.
38. Gissibl, T.; Thiele, S.; Herkommer, A.; Giessen, H. Sub-micrometre accurate free-form optics by three-dimensional printing on single-mode fibres. *Nat. Commun.* **2016**, *7*, 11763.
39. Rekštytė, S.; Jonavičius, T.; Malinauskas, M. Direct laser writing of microstructures on optically opaque and reflective surfaces. *Opt. Laser Eng.* **2014**, *53*, 90–97.
40. Malinauskas, M.; Žukauskas, A.; Hasegawa, S.; Hayasaki, Y.; Mizeikis, V.; Buividas, R.; Juodkazis, S. Ultrafast laser processing of materials: from science to industry. *Light Sci. Appl.* **2016**, *5*, e16133.
41. Menzel, R. *Photonics: linear and nonlinear interactions of laser light and matter*; Springer, 2001.
42. Kosareva, O.G.; Liu, W.; Panov, N.A.; Bernhardt, J.; Ji, Z.; Sharifi, M.; Li, R.; Xu, Z.; Liu, J.; Wang, Z.; Ju, J.; Lu, X.; Jiang, Y.; Leng, Y.; Liang, X.; Kandidov, V.P.; Chin, S.L. Can we reach very high intensity in air with femtosecond PW laser pulses? *Laser Phys.* **2009**, *19*, 1776–1792.
43. Panagiotopoulos, P.; Papazoglou, D.G.; Couairon, A.; Tzortzakis, S. Sharply autofocused ring-Airy beams transforming into non-linear intense light bullets. *Nat. Commun.* **2013**, *4*, 2622.
44. Point, G.; Brelet, Y.; Houard, A.; Jukna, V.; Milián, C.; Carbonnel, J.; Liu, Y.; Couairon, A.; Mysyrowicz, A. Superfilamentation in Air. *Phys. Rev. Lett.* **2014**, *112*.

45. Maximova, K.; Wang, X.; Balčytis, A.; Fan, L.; Li, J.; Juodkazis, S. Silk patterns made by direct femtosecond laser writing. *Biomicrofluidics* **2016**, *10*, 054101.
46. Selimis, A.; Mironov, V.; Farsari, M. Direct laser writing: Principles and materials for scaffold 3D printing. *Microelectron. Eng.* **2015**, *132*, 83–89.
47. Žukauskas, A.; Malinauskas, M.; Kontenis, L.; Purlys, V.; Paipulas, D.; Vengris, M.; Gadonas, R. Organic dye doped microstructures for optically active functional devices fabricated via two-photon polymerization technique. *Lith. J. Phys.* **2010**, *50*, 55–61.
48. Jonušauskas, L.; Lau, M.; Gruber, P.; Gokce, B.; Barcikowski, S.; Malinauskas, M.; Ovsianikov, A. Plasmon assisted 3D microstructuring of gold nanoparticle-doped polymers. *Nanotechnology* **2016**, *27*, 154001.
49. Leon-Saval, S.G.; Birks, T.A.; Bland-Hawthorn, J.; Englund, M. Multimode fiber devices with single-mode performance. *Opt. Lett.* **2005**, *30*, 2545–2547.
50. Thomson, R.R.; Birks, T.A.; Leon-Saval, S.G.; Kar, A.K.; Bland-Hawthorn, J. Ultrafast laser inscription of an integrated photonic lantern. *Opt. Express* **2011**, *19*, 5698–5705.
51. Meisel, D.C.; Diem, M.; Deubel, M.; Pérez-Willard, F.; Linden, S.; Gerthsen, D.; Busch, K.; Wegener, M. Shrinkage Precompensation of Holographic Three-Dimensional Photonic-Crystal Templates. *Adv. Mater.* **2006**, *18*, 2964–2968.
52. Maigyte, L.; Staliunas, K. Spatial filtering with photonic crystals. *Appl. Phys. Rev.* **2015**, *2*, 011102.
53. Rekštytė, S.; Jonavičius, T.; Gailevičius, D.; Malinauskas, M.; Mizeikis, V.; Gamaly, E.G.; Juodkazis, S. Nanoscale Precision of 3D Polymerization via Polarization Control. *Adv. Opt. Mater* **2016**, *4*, 1209–1214.